Tailoring Ag Electron-Donating Ability for Organohalide Reduction: A Bilayer Electrode Design

Ali Abbaspourtamijani 1† , Dwaipayan Chakraborty 1† , Henry Sheldon White 2 , Matthew Neurock 3 , Yue Qi 1 , *

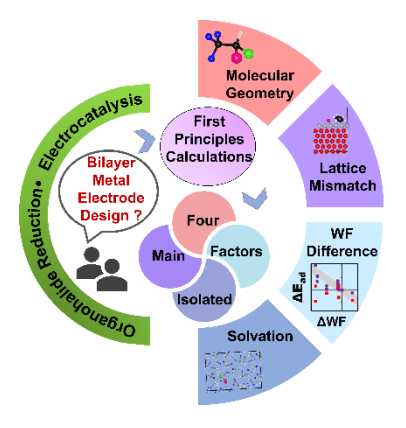
¹School of Engineering, Brown University, Providence, RI 02912, United States

²Department of Chemistry, University of Utah, Salt Lake City, Utah 84112, United States

³Department of Chemical Engineering & Materials Science, University of Minnesota, Minnesota, Minnesota 55455, United States

KEYWORDS: organohalide reduction, electrocatalysis, bilayer metal electrode, adsorption, work function, lattice mismatch, solvation effects, density functional theory

TOC graphic:



†These authors contributed equally

*Corresponding author: Y. Q. (yueqi@brown.edu)

Abstract:

Electrochemical reduction of organohalides provides a green approach in the reduction of environmental pollutants, synthesis of new organic molecules, and many other applications. The presence of a catalytic electrode can make the process more energetically efficient. Ag is known to be a very good electrode for the reduction of a wide range of organohalides. Herein, we examine the elementary adsorption and reaction steps that occur on Ag and the changes that result from changes in the Ag-coated-metal, strain in Ag, solvent, and substrate geometry. The results are used to put forth an electrode design strategy that can possibly be used to further increase the catalytic activity of pure Ag electrodes. We have shown how epitaxially depositing one to three layers of Ag on catalytically inert or less active support metal can increase the surface electron donating ability, thus increasing the adsorption of organic halide, and the catalytic activity. Many factors, such as molecular geometry, lattice mismatch, work function, and solvents, contribute to the adsorption of organic halide molecules over the bilayer electrode surface. To isolate and rank these factors, we examined three model organic halides, namely, halothane, bromobenzene (BrBz) and benzyl bromide (BzBr) adsorption on Ag/metal (metal = Au, Bi, Pt and Ti) bilayer electrodes in both vacuum and acetonitrile (ACN) solvent. The different metal supports offer a range of lattice mismatches and work function differences with Ag. Our calculations show that the surface of Ag becomes more electron donating and accessible to adsorption, when it forms a bilayer with Ti, since Ti has a lower work function and almost zero lattice mismatch with Ag. We believe this study will help to increase the electron donating ability of Ag surface by choosing the right metal support which in turn can improve the catalytic activity of the working electrode.

Introduction:

The reductive dehalogenation of carbon-halogen bonds plays a critical role in the catalytic abetment of environmental pollutants, organic synthesis, fundamental studies of electron transfer chemistry and in other fields^{1–4}. Reductive dehalogenation approaches, for example, are quite promising for the removal of toxic and very harmful chemicals such as polychlorobiphenyls (PCBs)⁵, chlorinated aliphatic hydrocarbons (CAHs)⁶, volatile organic compounds (VOCs)⁷, chloronitrobenzenes (CNBs)⁸ etc. This has prompted the tremendous recent interest in the electrochemical reduction of organohalides which involves the cleavage of carbon-halogen bonds under electrochemical conditions ^{7,9–11}. Current can be used as a green redox reagent or electron as a green reductant thus providing sustainable and clean avenues for organic electrosynthesis^{2,12,13}, pollution remediation^{1,14} etc. Electrochemical routes also help to avoid the use of hazardous reagents and the potential risk of secondary pollution^{1,2,15}. The practical realization of direct, selective, and energy efficient electrochemical dehalogenation of organohalides (by defeating the competing processes such as hydrogen evolution reaction or HER) over inert electrodes is difficult and will likely require the use of catalytic surfaces.^{16,17}

The use of a catalytic electrode (e.g. Ag), in place of an inert electrode (e.g. Glassy Carbon or GC), can significantly reduce the intrinsic energy barrier associated with the electron transfer to organohalides^{1,16} and thus reduce the overpotential. For example, the reported overpotential associated with the electron transfer for several aromatic bromide dehalogenations on Ag electrode is about 0.9 V lower than that on a GC electrode¹⁶. In a second example, associated with benzyl chloride reduction, there is a positive shift of 0.5 V in reduction potential reported for a Ag cathode with respect to the inert electrode¹⁸. This positive shift in potential also helps to suppress the side reactions. Thus, the design of electrodes with higher catalytic activity will help to enhance the applications of electrocatalytic dehalogenation.

While many catalysts have been used to carry out organic halide reduction, Ag, Cu and Pd are typically found to perform better than other metals^{4,7}. Ag, in particular, shows remarkable catalytic activity both in terms of positive shift of reduction potential and current efficiencies for a vast range of organic halides^{3,4,7,8,10}. An experimental study by Langmaier and Samec¹⁹, for example, shows that Ag sits at the top of the volcano plot for halothane reduction. Many efforts, such as structural or electronic modifications through engineering of size, morphology, doping, defect,

alloying, etc., have been made to further improve the catalytic activity for organohalide reduction in recent years^{20–24}. Some of such recent studies on deposited Ag electrodes^{25,26}, single atom catalyst surfaces²⁷, and atomically thin Pt film epitaxially grown on graphene²⁸ give rise to an interesting question: *can deposited Ag thin films or clusters on inactive electrode surface enhance the reduction performance of an otherwise inert electrode or even surpass the catalytic activity of the pure Ag itself*?

The idea of electrodeposition of silver working electrode on a support material for improved catalytic performance is borrowed from previous research from Bard et al.^{29,30}. who deposited Pt on Bi and examined changes in the hydrogen evolution reaction (HER) for various electrodeposited Pt sizes, ranging from a single atom to larger clusters. Various support electrode materials have been traditionally considered 'inert' as they are not expected to contribute directly to the reductive process of organic halides^{3,4}. However, it has been demonstrated that changing the support electrode materials can indirectly lead to changes in the reduction potentials of substrates (what is to be reduced)²⁹. Thus, depending on the different combinations of support and working electrodes, the substrate reduction potential may vary. There are still many open questions that remain regarding the specific roles of the working and supporting electrodes, solvent effects and potential approaches to enhance the catalytic performance of the Ag electrode. In this regard, a more detailed understanding of the influence of the electrode and solvent on the electrocatalytic processes is critical to advance further improvements.

Although limited, there are few experimental and theoretical studies that can be highlighted that attempt to deconvolute the multistep complex organohalide reduction processes^{11,19,31}. Previous studies on the dissociative electron transfer (DET) mechanism of electrochemical reduction of organic halides have shown the overall process to be a two-electron reduction process where the first electron transfer step was found to be the rate-limiting step (RDS)^{4,19}. The first step involving the carbon-halogen bond dissociation can either be stepwise or concerted in nature^{1,4,16,31}. The radical and halide ion are produced at the end of this step irrespective of the intermediate pathway. All of these previous studies also indicate that the synergy between the thermodynamic effect and the kinetic (mechanistic) effect dictates the catalytic activity of a material. The effect of electrode surface on the catalytic activity is linked through the molecular and dissociative chemical adsorption of the reactants, intermediates, and products, respectively^{11,19,31–34}. The sensitivity of

electrocatalysis on the surface adsorption has been confirmed via the volcano-shaped dependence of the catalytic activity for different materials obtained when plotted against the metal and relevant atomic (involving in creating the rate-determining critical bond) interaction^{19,35}. For example, in the case of halothane reduction, Langmaier and Samec obtained the volcano plot of the measured half-wave potential ($E_{1/2}$) of the reduction with respect to the Br-Metal bond strength¹⁴. Here we derived the half-wave potential, following Langmaier and Samec¹⁴, to be an explicit function of the equilibrium organic halide standard reduction potential, E^0 , the charge transfer rate, k^0 , and the surface adsorption coefficient, β . (More derivation details can be found in the Supporting Information, SI)

$$E_{1/2} = E^0 + \frac{RT}{\alpha F} \ln \left(\frac{nFAk^0}{m} \right) + \frac{RT}{\alpha F} \ln \left(\frac{2\beta^{1-\alpha}}{2+\beta c^0} \right) \tag{1}$$

where, n is number of electrons (n=1 for the first rate limiting electron transfer reaction), m is the mass transfer number, c^0 is the bulk concentration of organic halide, α is the charge transfer coefficient (which was reported as α =0.38, 0.73, 0.45, 0.19, 0.32 for Ag, Au, Cu, Ti, Hg respectively from measuring the halothane reduction on various rotating-disc electrodes in 1 M NaOH in methanol or water¹⁴), T is temperature. While E^0 can be predicted from first principles calculations³⁶, the adsorption coefficient, β , is related to the standard Gibbs energy of adsorption, ΔG_a^0 , which can be approximated to the first principles calculation predicted adsorption energy E_{ads} .

$$\beta = exp\left(-\frac{\Delta G_a^0}{RT}\right) \tag{2}$$

An understanding of the underlying mechanism and the influence of the atomic scale details on modulating the surface adsorption from first-principles calculations can thus be a very effective strategy to improve the catalytic activity.^{33,37}

In this context, the main objective of the current work is to isolate and understand the effects of molecular geometry, the lattice mismatch between the support and working electrodes, work function differences between the support and working electrodes, and the influence of explicit solvation in controlling the adsorption of specific organic halides on the electrode surfaces (hence the electron donating ability of the surface), and to provide the bi-metallic reduction reaction catalyst design rules. We will model Ag deposited on different metal electrodes, as epitaxial

Ag/metal (metal = Au, Bi, Pt and Ti) bilayer structures, as epitaxial growth is more likely when the deposited Ag films are only $1\sim3$ atomic layers thick or the Ag clusters are small. We propose ways to control the electrode reduction performance by varying the support metals for Ag. For this purpose, we have selected Au, Bi, Pt, and Ti as support metals. While Bi and Pt mismatch the lattice parameter of Ag and hence lead to more extended and compressed surfaces, respectively, when forming a bilayer with the working electrode; Au and Ti, on the other hand, have an almost negligible lattice mismatch with Ag. We can therefore begin to systematically probe the effect of lattice mismatch in different directions. We can also explore electronic differences as the work functions of Ti³⁸ and Bi³⁹ is lower than that of Ag⁴⁰, whereas those of Au⁴¹ and Pt⁴² are larger than that of Ag. This enables us to explore the effect of the work function difference on the surface adsorption or the electron donating ability of the Ag layer coupled with various support electrodes. In an effort to generalize our findings to a range of different organic halides, we have chosen halothane, bromobenzene (BrBz), and benzyl bromide (BzBr) as the organic halides to reduce. Our molecular choices are motivated by the fact that these species have been extensively researched for their reduction on different electrode surfaces^{3,19,43,44}. In addition, these three organic substrates take on different various geometric structures; halothane has a prismatic structure while bromobenzene and benzyl bromide possess an aromatic ring and can assume flatlying configurations when interacting with the electrode surfaces. Thus, we believe our choice of molecules can assist us in scrutinizing the effect of molecular structure on the adsorption and the easiness of the reduction process.

Materials and Methods:

First principles cluster and periodic calculations were carried out to predict the reduction properties of the molecules (halothane, BrBz and BzBr) and their adsorption on metal electrode surfaces (pristine Ag, Au, Bi and Pt and Ag/metal; metal = Au, Bi, Pt and Ti; bilayers), respectively. Density functional theory (DFT) based molecular calculations, i.e., geometry optimizations of the three candidate molecules and the absolute reduction potential calculations were carried out using the Gaussian 09 package^{36,45,46}. The solvent effect was examined by using the SMD implicit solvent approach. Periodic calculations including the geometry optimizations of the pure metals and various bilayers, the adsorption energy of the three substrates, and work

function calculations were carried out using the plane wave DFT package VASP^{47–49}. To model the explicit solvation calculations in the periodic systems we have first employed the MD simulation as implemented in the Forcite module of Materials Studio⁵⁰ to determine the solvent structure of acetonitrile at 25°C. The optimized solvent structures were then used in the VASP calculations to calculate the adsorption energies of halothane on Ag surfaces. Further details regarding the calculation details can be found in the SI.

Results and Discussions

Choice of the Systems:

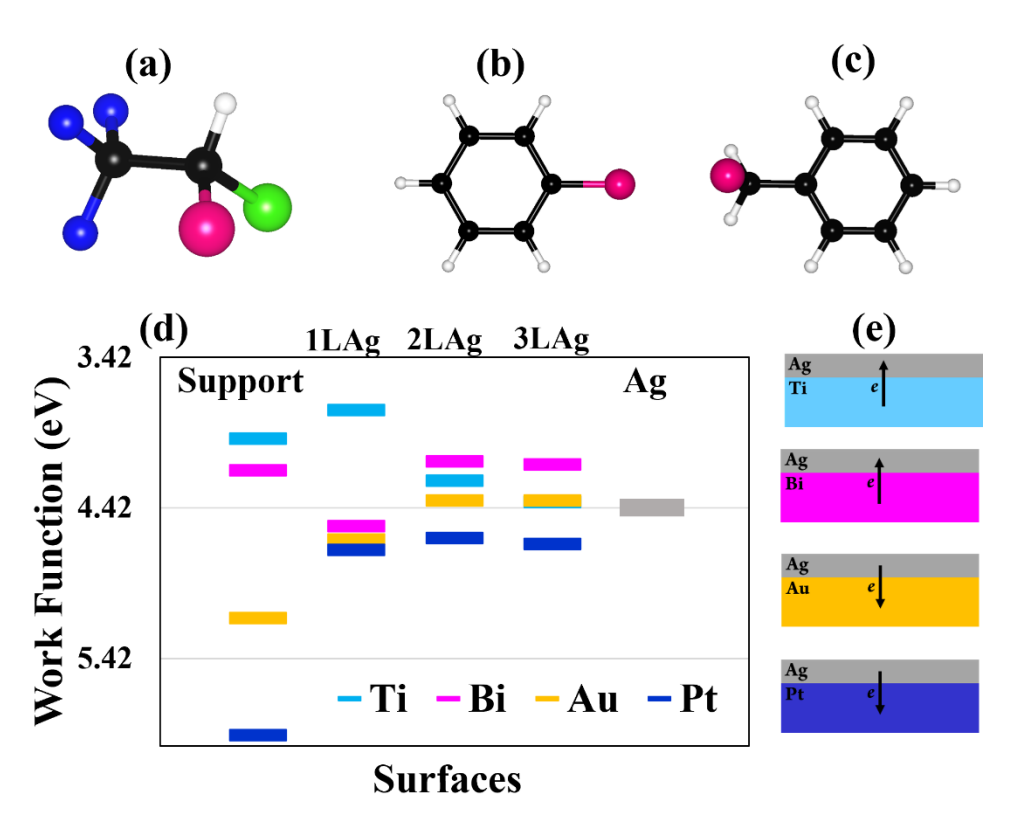


Fig 1: Relaxed structures of the: (a) Halothane, (b) BrBz, and (c) BzBr organic halides that are reduced where the black, white, magenta, blue, and green balls represent C, H, Br, F, and Cl, respectively. (d) The computed work function for different electrode surfaces (orientations shown in Table 2). (e) Expected electron transfer direction between the working Ag electrode and the support electrode in different bilayers.

To help advance the impact of our study, we have chosen alkyl halide (halothane), aromatic halide (BrBz) and benzyl halide (BzBr). Different organohalides can undergo different dehalogenation

mechanisms including stepwise as well as concerted dehalogenation depending on their molecular and electronic structures^{4,11}. We diversified our choice of support electrode materials by choosing metals with larger and smaller lattice parameters and work functions than those of the working electrode. We discuss the implications of the choice of our systems in detail below.

The organic halides and their reduction voltage:

Table 1: DFT computed reduction potentials of organic species (vs. SCE). E_{DFT}^0 is close to the standard reduction potential E^0 in Equation 1. Experimental data are based on Ag electrode in acetonitrile solvent.

	E_{DFT}^0 for the First	E_{DFT}^{0} for the Second	Experimental Reduction		
	Reduction (V)	Reduction (V)	Potential (V)		
Halothane	-1.11	-0.16	-1.12 ⁵¹		
BrBz	-2.14	-0.05	-1.81 ³		
BzBr	-1.24	-1.08	-1.05 ⁵¹		
Acetonitrile	-3.02	-	-3.00		

The DFT calculated first and second electron reduction potentials (See SI for computational details) which can be considered close to the standard reduction potential (E_{DFT}^0) as activity is treated as unity here are summarized in Table 1. The first reduction of the different halothane and BzBr substrates resulted in the direct cleavage of the C-Br bonds upon reduction to -1 state, resulting in the formation of CF₃CHCl• and C₇H₇• radicals, along with Br- anions. This occurs as the electron that transfers to these species adds to the LUMO of these molecules which involve a σ^* molecular orbital that is localized around the C-Br bond¹¹. BrBz, on the other hand, does not undergo automatic C-Br bond breaking upon its initial reduction. The second reduction of these halides was calculated by starting with the optimized structures obtained from the first reduction calculations as the initial structures. The second reduction potentials for halothane and BzBr were calculated starting with the free radical (R·) produced after the dehalogenation that occurred in the first reduction step to form the anion R^- using the free energies of $R^- + e \rightarrow R^-$. The second reduction of BrBz was calculated instead using the -1 charged BrBz anion as the initial structure (Table 1). In the second reduction of BrBz, the C-Br bond dissociated to form BrBz anion. It is welldocumented that the first reduction step is the RDS for the dehalogenation of these halides^{4,19}. Our results reported in Table 1 are fully consistent as all the second reduction potentials are less negative than the primary reduction potentials for these molecules. As such, we can infer that the second reduction steps are more thermodynamically 'likely' to occur. We have also calculated the first reduction potential for acetonitrile, which is generally the solvent used in organic halide reduction experiments. Upon reduction, the C-C=N bond of the acetonitrile takes on a bent structure such that the ∠C-C=N is reduced from 179.95° in its neural form to 128.52° in its reduced form. However, no bond breaking is observed in the acetonitrile molecule confirming the electrochemical stability of the solvent within the applied electrochemical potential window.

The DFT calculated first reduction potentials are, in good agreement with experimental data. The experimental values given in **Table 1** are reported as peak potential, whose difference with the half-wave potentials (vs. SCE) is much less (~ 0.03 V) than the DFT calculation error bars. As such, we approximate the peak potentials as the half-wave potential ($E_{1/2}$) in Equation (1). As discussed in the introduction, the half-wave potential contains both thermodynamic (equilibrium potential) as well as kinetic information. Since the Ag electrode is reported to demonstrate the fastest kinetics (closest values to the equilibrium potential), we selected it to carry out our current study¹⁹. The DFT-predicted reduction potentials for halothane are almost error-free compared to the experimental peak-potentials. While the value for BrBz is the farthest from its experimental counterpart with a difference of ~ 0.3 eV, it is in the reported range of errors for DFT-calculated free energies. ^{52,53} The slightly higher discrepancy on BrBz may come from kinetic reasons as well.

The metallic electrodes and their lattice mismatch and work functions:

Table 2: List of the calculated parameters (*viz.* lattice parameters and work functions) of electrode materials that can influence the organic halide reduction performance.

Bulk			Slab					
Symmetry	а (Å)	c (Å)	orientation	Supercell	A (Å)	<i>B</i> (Å)	Ag Lattice Mismatch	Work function (eV)
FCC	4.07		Ag (111)	$3\sqrt{3}\times3$	14.95	8.63	-	4.42
FCC	4.10		Au (111)	$3\sqrt{3}\times 3$	15.08	8.70	+0.81%	5.3
P63/mmc	4.53	11.69	Bi (001)	$2\sqrt{3} \times 2$	15.68	9.05	+4.61%	4.17
FCC	3.93		Pt (111)	$3\sqrt{3}\times 3$	14.44	8.34	-3.41%	5.93
P63/mmc	2.93	4.66	Ti (001)	$3\sqrt{3}\times3$	14.96	8.64	+0.07%	3.96

In analyzing the influence of bilayer electrode catalyst structures where Ag is deposited on the surface of the support electrode, we need to consider two main factors: a) The lattice mismatch between the support and Ag; and b) the work functions difference between the support and Ag. Au, Bi, Pt, and Ti metals were chosen as different supports as they reflect a range of differences in both their lattice constants and work functions as compared to Ag as mentioned earlier.

The DFT calculated lattice parameters for each metallic electrode material reported in **Table 2** are in excellent agreement with their experimental values (Tables S1 in SI). It can be assumed that Ag layers initially grow epitaxially when ultrathin deposition (one to three layers) on the support is considered. The Ag-deposited-metal electrodes were modeled here as Ag deposited on metal slabs with common supercell dimensions ($3\sqrt{3} \times 3$) as listed in Table 2 with the exception of Bi which is ($2\sqrt{3} \times 2$). The results show that the silver lattice undergoes an expansion when deposited onto Au as well as Bi, but contracts when deposited on Pt. The lattice mismatch between Ag (111) and Ti (001) is a minimum.

Table 2 also listed the calculated work functions of pure metals. The calculated Ag (111) work function is larger than those for Ti (001) and Bi (001), and smaller than those for Au (111) and Pt (111). Thus, when Ag is deposited onto a Ti or Bi support, electron transfer is expected to occur from Ti or Bi to Ag. This would make the working electrode more electron donating. On the other hand, in the case of Ag on Au and Pt support electrodes, the electron transfer direction is reversed, where a less-electron donating silver electrode is expected to form (Scheme shown in Fig 1e). These expected trends were confirmed in computing the work functions for various heterostructures (see Fig 1d and more detailed discussions in **Section 3.2.B**).

Adsorption and Decomposition of the organic halides on pristine metal surfaces:

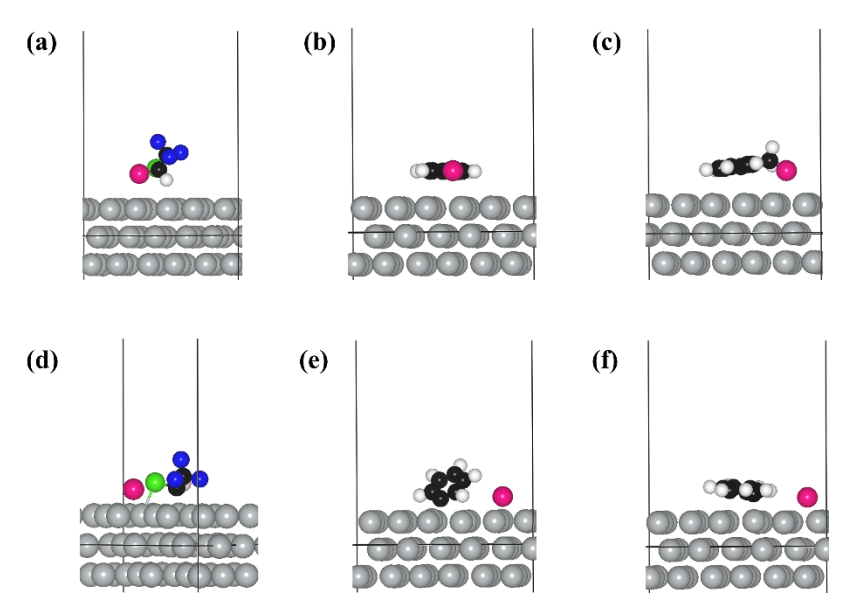


Fig 2: Molecular and dissociative adsorption of (a) & (d) Halothane, (b) & (e) BrBz, and (c) & (f) BzBr molecules on pure Ag (gray balls) surface.

The adsorption coefficient, β , in the analytical model for the half-wave potential in Equation 1 depends on the electrode-molecule interactions (Equation 2), which can be calculated directly with DFT. The type/shape of the molecule, its adsorption mode/configuration, and packing density collectively determine the molecule's adsorption energy. Here, we first discuss the adsorption energies in a vacuum. In the case of BrBz adsorption on Ag(111), the flat-lying configuration where the BrBz π -bonds to the Ag surface was calculated to be more stable than the upright configuration (with Br pointing towards the hollow surface site) by 0.52 eV (Figure S3 in SI). Therefore, multiple initial adsorption configurations have always been tested and only the lowest energy configurations are reported. Three different adsorption behaviors have been observed after DFT relaxation. On the Pt (111) surface, halothane undergoes physical adsorption with a calculated adsorption energy of E_{ad}=0.96 eV. BrBz adsorption, on the other hand, undergoes chemisorption as reflected in the significant structural distortion on the surface and strong adsorption energy of E_{ad}=2.17 eV. These molecules have never been observed to undergo automatic carbon-halogen bond dissociation under any condition. The adsorption of BzBr on Pt(111), however, differs from the halothane and BrBz adsorption in that the C-Br bond dissociates upon adsorption leading to the formation of both adsorbed Br and adsorbed benzyl group on the surface depending upon the strength of interaction between the molecule and the surface (distance from the surface) (Figure

S4 in SI). We have also observed direct C-Br bond breaking upon adsorption for halothane on Ag (Figure S5 in SI). Although BzBr did not undergo spontaneous C-Br bond breaking upon its adsorption to Ag, manual dissociation of the C-Br bond resulted in a more stable adsorbed state (by 0.83 eV) (Figure S5 in SI). Doubling the simulation cell laterally effectively reduced the intermolecular adsorbate interactions on the surface and in turn increased the adsorption energies but did not change the adsorption states (such as the chemical, physical, or bond dissociated) configurations (further discussed in the SI).

Therefore, for comparison, we examined two different types of adsorption states, namely, the molecular state in which the C-Br bond is intact, and the dissociative state where the C-Br bond is cleaved on different substrates. These results are collected in **Table 3**. The strongest binding for the molecular adsorption was for BrBz on Pt (2.17 eV) and the strongest binding for the dissociative adsorption was for BzBr also on the Pt surface (4.46 eV), due to the coupling between the adsorbate valence states and the metal d-states³³. While a favorable binding energy is desired for the catalytic surface, too strong of binding can in fact 'poison' the electrode surface and limit catalytic activity (as per Sabatier principle⁵⁴). Therefore, an intricate balance of the interactions is required for optimal adsorption energy at the electrode surface. Given the excessively strong adsorption of dissociative BzBr on Pt, this surface is very likely not an 'ideal' choice for promoting BzBr reduction process.

One can think of molecular adsorption as the first step, followed by the dissociation of the C-Br bond corresponding to the first electron transfer reduction of the organic halides. The Br adsorbed on the metal surface is negatively charged (according to the Bader Charge analysis given in Table S2 in SI). While we have not explicitly separated out the electron transfer, the stronger dissociative adsorption can be viewed as a strong driving force for the first electron reduction and bond dissociation. Interestingly, Ag shows a large driving force for halothane and BzBr reduction while Bi shows just the opposite. Therefore, it can be expected that Bi would be a rather 'inert' electrode for these reduction reactions. The results for BrBz adsorption on the different metals indicate that the BrBz does not undergo spontaneous cleavage of the C-Br bond upon adsorption. This is consistent with the minimal increase in the adsorption energy for the dissociated state over the molecular state on all the metals. The calculated adsorption energy trends discussed are consistent with experimentally reported reduction voltages on different electrodes in general.⁵¹

Table 3: Adsorption energies for halothane, BrBz, and BzBr on different substrates (eV) (- means no intact configuration can be found).

		Adsorption Energy (eV)					
		Halothane		BrBz		BzBr	
Electrode		molecular	dissociative	molecular	dissociative	molecular	dissociative
Pure metal	Pure Ag	0.6	1.63	0.94	1.15	1.00	1.83
	Pure Au	0.56	0.89	0.96	0.70	1.03	1.35
	Pure Bi	0.41	0.33	0.52	0.46	0.52	0.16
	Pure Pt	0.96	2.76	2.17	2.31	1.21	4.46
Strained Ag	+0.81% (to Au)	-	1.67	0.94	1.05	1.1	1.86
	+4.61% (to Bi)	-	0.69	0.97	1.32	0.99	2.06
	-3.41% (to Pt)	-	1.33	0.90	0.86	0.99	1.46
Ti support	1L Ag on Ti	-	2.79	1.22	2.16	1.05	2.89
Au support	1L Ag on Au	-	1.76	0.97	1.19	1.07	1.97
	2L Ag on Au	-	1.76	0.96	1.17	1.08	1.98
	3L Ag on Au	-	1.66	0.99	1.26	1.10	2.1
Bi support	1L Ag on Bi	-	1.24	0.78	0.67	1.53	1.75
	2L Ag on Bi	-	1.13	1	0.94	-	2.57
	3L Ag on Bi	-	1.80	1.07	0.55	1.14	2.24
Pt support	1L Ag on Pt	-	0.53	1.06	1.24	1.26	2.04
	2L Ag on Pt	_	1.24	0.96	1.09	1.07	1.85
	3L Ag on Pt	-	1.55	0.99	1.01	1.09	1.84

Strain Effect due to lattice mismatch

To isolate the effects of lattice expansion and contraction on the adsorption energy, we have increased and decreased the lattice dimensions of the freestanding Ag slab to match those of Au, Bi, and Pt, and recalculated the adsorption energy of halothane, BrBz, and BzBr on each of those dimensionally modified Ag surfaces (Table 2). The changes in the molecular adsorption energies were found to be much less sensitive to lattice strain of Ag than dissociative adsorption energies. In all the cases, the spontaneous C-Br bond dissociation upon adsorption is restored. Overall, halothane was calculated to be much more sensitive to the change in the lattice dimensions than BrBz. For example, the dissociative adsorption energy of halothane was reduced by a factor of 2 when the Ag lattice was expanded by \sim 5% (to match those of Bi). However, the same change in Ag lattice dimensions only resulted in an increase of \sim 7-12% in the dissociative adsorption energies for BrBz and BzBr. On the other hand, compressing the Ag lattice dimensions by \sim 3.4% (to match those of Pt) resulted in a \sim 20% dissociative adsorption energy reduction for all. The Ag and Au lattice mismatch is < 1%. As such there is a negligible change of adsorption energy (less than \sim 0.04 eV) when Ag lattice is expanded to match with that of Au. As shown in Fig 2, for both BrBz and BzBr, the benzene ring lies flat on the metal surface (*viz.*, molecular adsorption) and the

shared π -bond that forms between the aromatic and metal surface is not significantly affected by lattice strain. In comparison, the linear halothane interacts with the metal via a prismatic upright adsorption state on the surface before C-Br bond breaking. In this case, lattice strain alters both the bond length and bond angles and thus impacts the adsorption energy more significantly. This is another manifestation of the fact that the type/shape of the molecule plays an important role in the adsorption strength.

Effect of work function (WF) change (via -BrBz and BzBr Adsorption):

The electrodes work functions were found to be very sensitive to forming a bilayer with Ag. Even depositing a single monolayer of Ag significantly altered the WF of the electrode surface as compared to the pure metals, as shown in Fig 1d. While increasing the number of Ag layers tends to resemble a pure Ag-like behavior, the Ag-deposited-electrode surfaces still show differences in their WFs compared to pure Ag due to the formation of heterogenous metal junctions (shown in Fig 1e). Expanding the Ag lattice by ~5% (to that of Bi) and contracting Ag lattice by 3.4% (to that of Pt), lead to changes in the work function of -0.13 eV and +0.14 eV, respectively. Thus, the isolated straining effect due to lattice mismatch on work function is rather small. More dramatic changes come from the formation of bimetallic heterojunctions. Due to WF differences between Ag and the support, the Ag WF would decrease on Ti and Bi supports but increase on Au and Pt supports. Therefore, the Ag surface on Ti and Bi supports is expected to become more electron donating than pure Ag. The difference in work function between the working electrode and support electrode can be viewed as a pre-applied voltage on the working electrode. If the pre-applied voltage has the same direction as the external applied voltage (e.g., more negative for the reduction reactions), it will enhance the reaction with a lower applied voltage. The calculated WFs shown in Fig. 1 for a monolayer of Ag deposited on the different supports, however, do not necessarily always follow these trends. For example, one layer (1L)-Ag deposited Bi surface shows a higher WF than that of pure Bi and Ag (as shown in Fig 1d and Table S3 of SI). However, 1L-Ag deposited on a Ti surface was calculated to be lower than the WFs for Ti and Ag. Work functions have also been found to be affected by lattice mismatch. This may play a role in the 1L-Ag deposited Bi case. Now, as Ag and Ti surfaces are effectively mismatch-free, it is an ideal system to investigate the role of surface work function on the surface adsorption of organic halides. We

therefore only investigated the one Ti-containing heterostructure that has a significantly lower work function than pure Ag: 1LAg + Ti.

The work function change on the Ag-deposited-electrode surfaces is likely to impact the reduction reactions. Since the adsorption of BrBz and BzBr has been found to be less sensitive towards lattice mismatch, both in their molecular and dissociated forms (as seen in **Table 3**), they are expected to serve as the best candidates to isolate the impact of the work functions on reduction reactions.

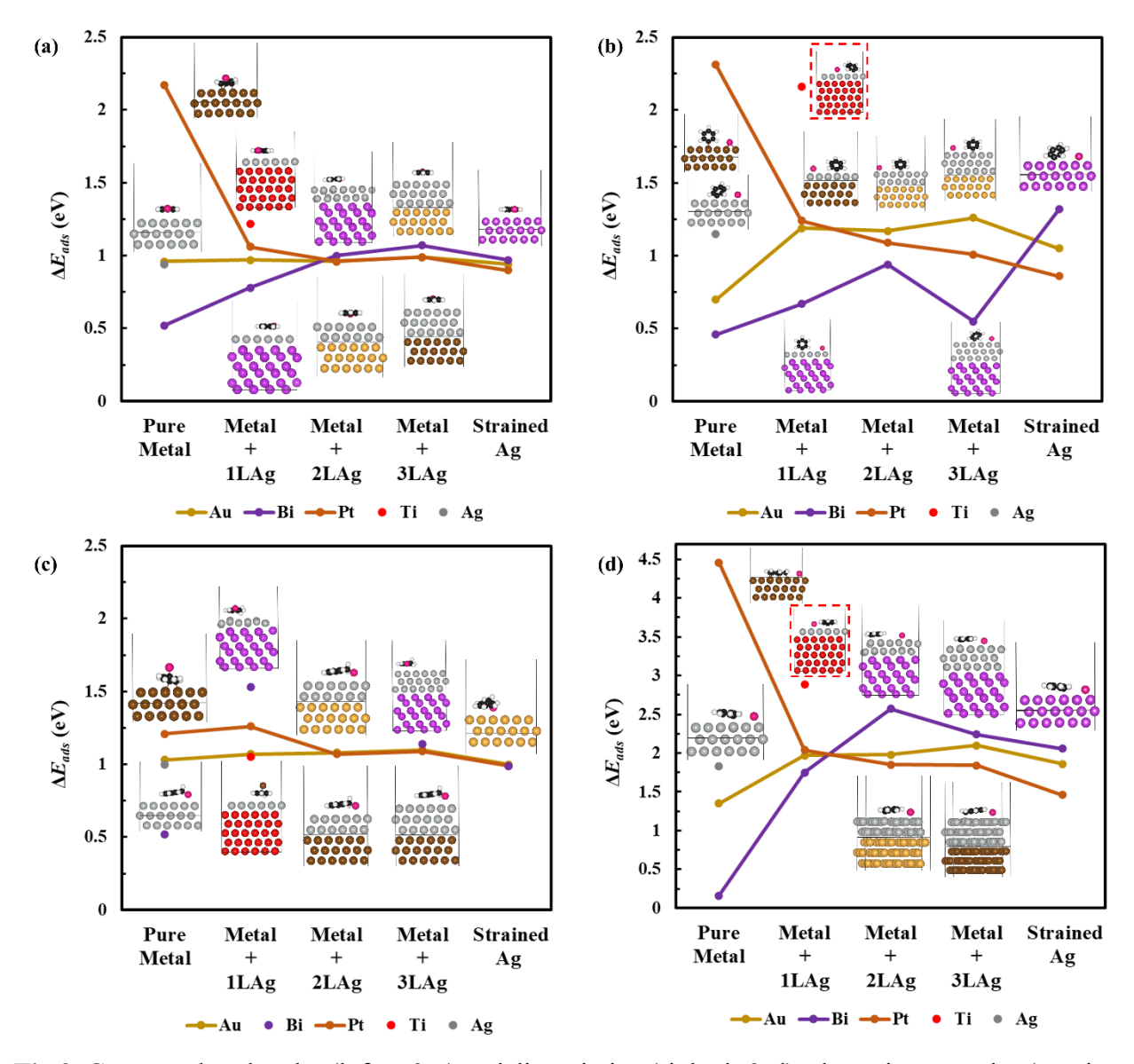


Fig 3: Computed molecular (left, a & c) and dissociative (right, b & d) adsorption energies (starting with manual dissociation where needed) and side views of selected structures of BrBz (top panel, a & b) and BzBr (bottom panel c & d) on Ag deposited metal supports (heterostructures with Au, Bi, Pt and Ti). The gray colored Ag is pure silver, while Ag with other colors denotes the strained

silver (purple means Ag strained to Bi lattice parameter, golden means Ag strained to Au lattice parameter). The effect of dissociative adsorption energy enhancement is highlighted in the red rectangles.

Fig 3 shows the molecular and as well as dissociative adsorption energies of BrBz and BzBr on one to three layers of epitaxially grown Ag film on pure metal supports (Au, Bi, Ti and Pt), and the same on both pure and strained Ag electrodes. Fig 3 also includes the adsorption energies for the pure support electrode metals (Au, Bi and Pt). The results show that even a monolayer of Ag can dramatically shift the adsorption energy of an otherwise 'inert' (e.g., Pt) or less active electrode to a more Ag-like electrode. For all supports an Ag-like behavior was observed up to 3 layers of Ag on different metal supports, especially the molecular adsorbed cases. The dissociative adsorption energies show more dramatic changes on Ag-deposited supports. In most cases, Agdeposited-metal surfaces further stabilize the dissociative adsorbed states compared to the molecular adsorbed states, indicating enhanced driving force for reduction and C-Br bond breaking. For all the Ag thicknesses the dissociative adsorptions are energetically more favorable than molecular adsorptions on these supports except BrBz on Ag-Bi surfaces. The molecular adsorption of the BzBr and BrBz on all the surfaces examined all result in π -bound state where the aromatic lies flat along the surface as seen in Fig. 3. The resulting benzyl intermediate that formed upon the dissociative adsorption of the BzBr also lies parallel to the surface for all metals. All the aryl radicals that formed, on the other hand, sit upright on the surface in order to complete the sp² bonding of the undercoordinated C atom in aryl ring.

The change in the adsorption energies on the different Ag-deposited-metal supports are further correlated with the WFs of these bilayer structures with respect to pure Ag as shown in **Fig 4**. Although not a perfect correlation, an overall enhancement in the adsorption energetics is observed on surfaces with reduced work functions, such as on Bi and Ti, as the Ag surfaces become more electron donating upon the formation of heterostructures with these metals. Au-supported Ag bilayers were found to be the least sensitive to Ag thickness. This is due to the small change in work function upon the formation of heterostructures and the result of the minimal lattice mismatch between Au and Ag. 1L Ag-deposited-Ti support was used as a testing case since it has the lowest WF and almost perfect lattice match with Ag. As a result, there were significant increases in adsorption energies on 1L-Ag deposited Ti in the dissociative adsorption of BrBz

(2.00 eV vs. 1.15 eV on pure Ag), and BzBr (2.89 eV vs. 1.83 eV on pure Ag), and even in the molecular adsorption of BrBz (a 0.28 eV increase) compared to pure Ag. Again, this is attributable to the large work function differences between pure Ag and its heterostructure with Ti.

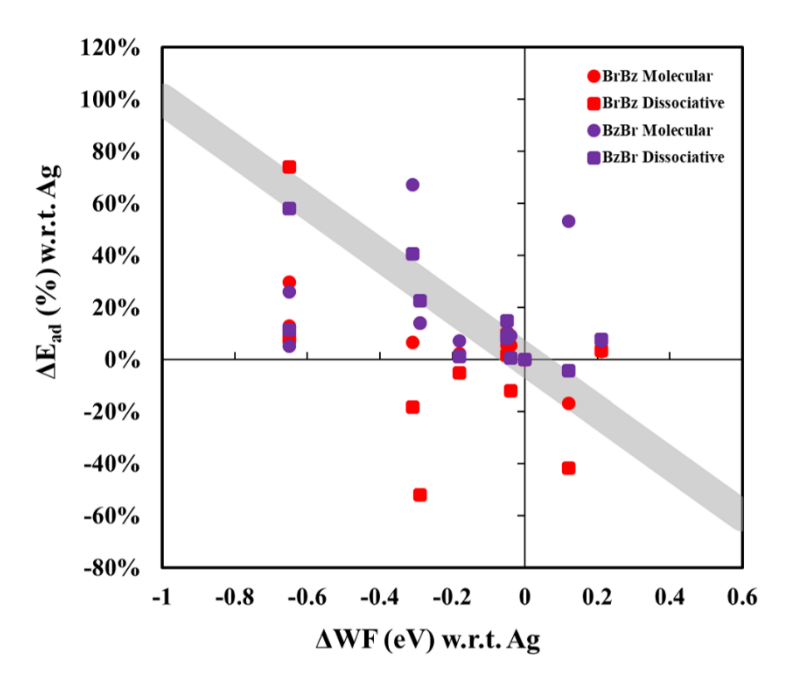


Fig 4: Correlation of change of adsorption energy on Ag-deposited metal surfaces with work functions. The gray line is to guide the eyes.

The combined strain and work function effect on Halothane reduction Ag-modified electrode surface:

Next, we examined the adsorption of halothane on pure metal and modified surfaces. The results are shown in **Fig 5**. A few interesting observations can be made in these cases. Unlike the previously studied BrBz and BzBr aromatic molecules, halothane spontaneously resulted in C-Br bond breaking (activity) on the Ag-deposited heterostructures. The pure support metals, on the other hand, did not show any activity for halothane following the previous trend shown for the BzBr and BrBz substrates. Again, manual dissociation of C-Br bond in halothane leads to more stable dissociative adsorption energy than molecular adsorptions for pure Au and Pt, but not on pure Bi. Given the fact that lattice strain or lattice mismatch was larger for the halothane adsorption than the two aromatic halide and benzyl halide studied due to the molecular geometry as discussed

earlier, we believe, in case of halothane adsorption it is hard to isolate the staining and WF effect (as we did for BrBz and BzBr) and the observations made in course of halothane adsorption are the results of the combination of both the effects.

Thus far, we have put forward three main factors that influence the strength of adsorption: shape/type of molecule, lattice strain, and WF. An intriguing question to be posed now is how do these factors operate in aggregate? To answer this question, we believe halothane is the ideal candidate for the reasons discussed in the previous paragraph.

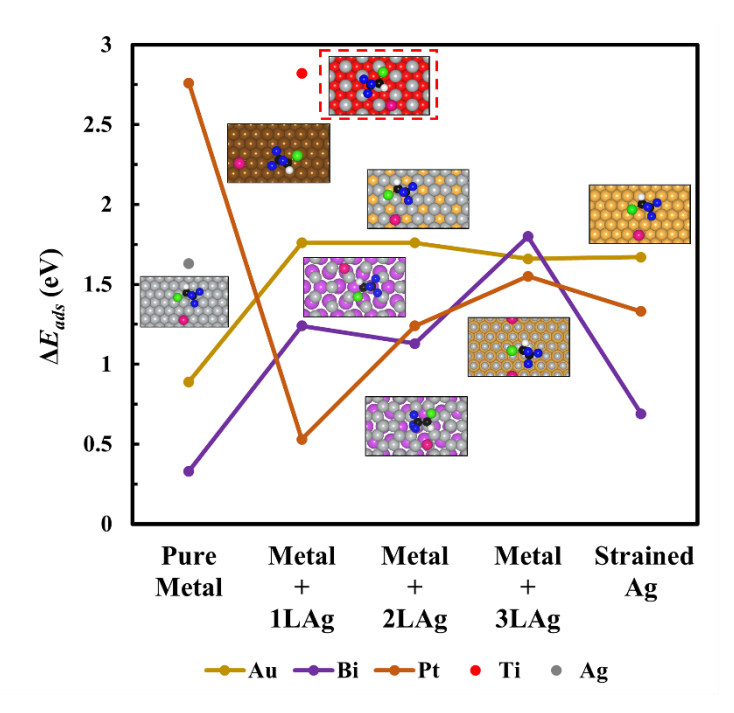


Fig 5: Computed dissociative adsorption energies (starting with manual dissociation where needed) and top views of selected structures of halothane on Ag-deposited metal supports (heterostructures with Au, Bi, Pt and Ti). The gray colored Ag is pure silver, while Ag with other colors denotes the strained silver (golden means Ag strained to Au lattice parameter). The effect of adsorption energy enhancement is highlighted in the red rectangle.

In the case of Ti and Au heterostructures with Ag, we would expect that the adsorption phenomenon is primarily dominated by the metal's WF, even in the case of halothane, as these two metals have very similar lattice constants with Ag and show minimal lattice mismatch. With a single layer of Ag deposited on Au, the work function difference indeed decreases the adsorption

energy. However, at 2 and 3 layers of Ag deposited on Au, the adsorption energy is as strong as free Ag. This is consistent with the fact that the work function of the heterostructure is very close to that of Ag (**Fig 1d**). This is also true for all heterostructures deposited with 3 layers of Ag. The greatest enhancement in the adsorption energy was observed for 1LAg + Ti, for which the adsorption energy is 2.79 eV, and is accompanied by C-Br dissociation. This stronger adsorption is due to the low work function for 1LAg + Ti heterostructure, which leads to enhanced electron donating ability of the bilayer electrode.

Interestingly we found, for Bi support, two competing effects dictate the adsorption energy of halothane. On one hand, the Bi support lowers the work function of the heterostructure, thus making the deposited-Ag-surface more favorable for stronger adsorption. On the other hand, lattice mismatch effect (as shown in section 2.2.A.) decreases the tendency of Ag surface to bind the halothane. For 1 and 2 layers of Ag on Bi, the former effect dominates whereas for 3 layers of Ag the latter effect dominates. For the Pt support, both work function differences and lattice mismatch act unidirectionally, ruling for a weaker adsorption on 1 and 2 layers of Ag deposited on Pt. Whereas, at 3 layers of Ag deposition, the behavior begins to mimic that of free Ag.

Solvation effects:

Heretofore, all of the calculations were carried out in vacuum, in the absence of solvent. In practice, the electrocatalytic experiments conducted for organic halide reduction are generally carried out in organic aprotic solvents such as acetonitrile. The effect of solvation on the adsorption energies in this study was modeled with a thermodynamic cycle derived by Phongpreecha et al.⁵⁵. The modified adsorption energy in solvent can be expressed as:

$$E_{ads}^{solv.} = E_{ads} - (1 - \delta) E_{solv.} - \theta E_{ads}^{l}$$
 (3),

where E_{ads}^{solv} is the adsorption energy after including the solvent effects. E_{ads} is the adsorption energy in vacuum (see equation S1 in SI). E_{solv} and E_{ads}^{l} are the solvation energy of the adsorbate and the adsorption energy of solvent on the adsorbent surface, respectively. Finally, δ is the fraction of solvation area retained and θ is the fraction of the surface area lost after the adsorption moves from a fully solvated state to an adsorbed state in the liquid phase⁵⁵. Following this approach, we have recalculated the adsorption energetics of halothane on various heterostructure surfaces (as shown **Fig 6**).

20

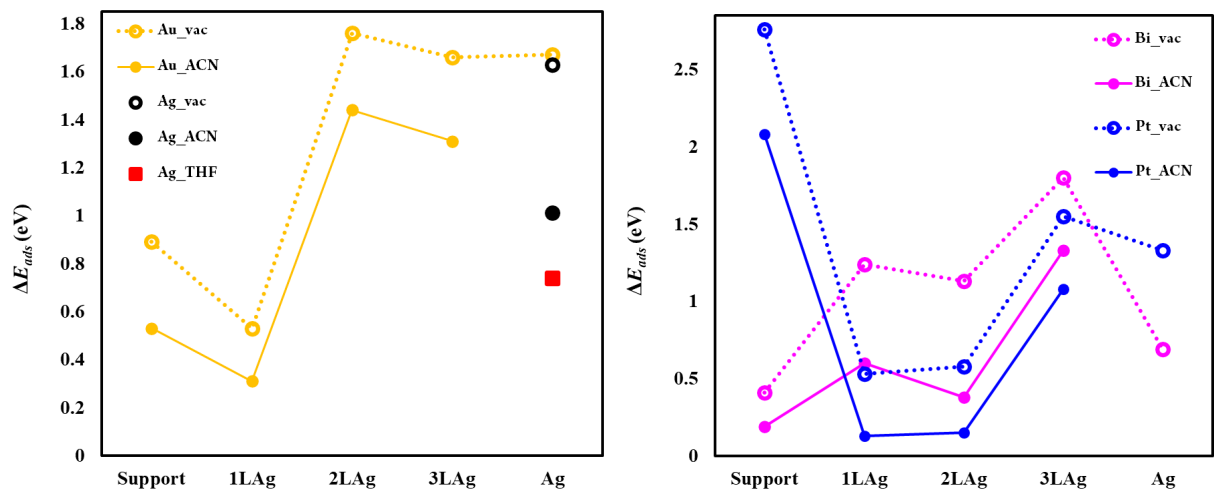


Fig 6: Eads of halothane on Ag + Au (left), and on Ag + Bi and Ag + Pt (right) in vacuum and solvated environments.

These additional calculations show that overall, adsorption energies are systematically reduced as compared to their vacuum counterparts. This is due to the attractive interactions between the solvent (acetonitrile) and the solute (halothane) and the solvent and the electrode surface (e.g., Ag), both of which act to counterbalance the attractive forces between the solute (adsorbate) and the electrode. Langmaier and Samec have shown that a less polar solvent makes the reduction process of halothane less energetically favorable¹⁹. Herein, we examined this effect by changing the solvent from acetonitrile ($\varepsilon = 37.5$) to THF ($\varepsilon = 7.6$). As a result, the adsorption energy of halothane on a freestanding Ag surface in acetonitrile (1.01 eV) was reduced to 0.74 eV on the Ag surface in THF. Given that the reduction process is surface mediated, the decrease in the adsorption energy that resulted in moving to a less polar solvent can lead to less electrocatalytic activity and ultimately a larger overpotential. This is in qualitative agreement with Langmaier and Samec's findings. The systematic decrease in the adsorption energy also moves the adsorption energetics closer to a more 'reasonably expected' range of 1-2 eV per molecule, which is also evidence that a more realistic picture is provided through the lens of solvation. While the quantitative adsorption energies are weaker than those in the gas phase, the overall trends in the liquid phase remain the same as those in the gas phase. We have therefore concluded that while including solvent effects changes the absolute values of adsorption energies, it does not alter the trends observed in vacuum

for benzyl bromide or bromobenzene as well. As such, we discontinued our investigations of the solvent effects at this point.

Design Rules:

Leveraging what we have learned so far, we propose here a set of design rules for constructing bilayer metal electrodes. Our primary focus is to establish an initial set of guiding principles to aid in systematically choosing the support electrode to tune the catalytic activity of the working electrode (Ag) as needed.

- I. Different organic halides show different responses to the changes in lattice. Alkyl halide molecules typically exhibit more sensitivity to the metal surface than aromatic molecules which lie flat and π -bond to the surface. The adsorption mode of the molecules also dictates their interaction strength with the surface where physiosorbed intermediates are more weakly bound than those that chemisorb and dissociate.
- II. Lattice mismatch between the working electrode and support electrode strongly affects the dissociative adsorption but does so in a complex way where the adsorption strength depends on the type/shape of the molecule and the nature of the tensile or compression strain. Minimizing the extent of mismatch is helpful in achieving a more controllable adsorption process.
- III. A more reductive electrode surface can be attained by using a support electrode with a work function that is smaller than that of the working electrode (e.g., Ti). The opposite effect can be used to obtain a less reductive surface (e.g., Pt).
- IV. Solvent effects systematically decrease the tendency of electrode surfaces to bind molecules. In order to predict the strength of adsorption on the surface in the presence of solvent, one should consider, at the least, using a scaling factor to account for this decreased tendency.

Based on these rules, we have proposed Ti as one viable candidate. The (0001) plane of Ti has almost no lattice mismatch (-0.04 %) with respect to our working Ag electrode (statement II). Furthermore, the Ti work function (3.96 eV) is significantly lower than that of Ag (statement III). We, therefore, expect the Ag surface to become more readily capable of donating electrons (adsorbing molecules) in the presence of Ti as the support electrode. As seen in Table S3 in SI, the addition of the first layer of Ag on the Ti support electrode results in an overall work function that

is significantly lower than that of free Ag. At three layers of Ag, however, the overall work function is closer to that of free Ag. This demonstrates why we would expect to see an increase in the adsorption energies, especially for a heterostructure with one layer of Ag on Ti. Compared to Ag, Ag + Ti adsorption energies are significantly stronger for dissociative cases. This shows that the difference in work function is ultimately the determining factor for Ag + Ti, as it makes the Ag surface far more electron donating than the freestanding Ag surface. Using the abovementioned criteria, we have been able to predict a stable support electrode (i.e., Ti) that can enhance the adsorption behavior of the Ag electrode. It is important to note here that in practice the catalytic activity of electrodes for organohalide reduction depends on a number of factors such as the strength of adsorption, the surface coverage, and the rate of desorption of reactant, intermediate, product, and solvent molecules as well as a range of other factors. .11,32,34,56 As a result, enhancement of the dissociative adsorption behavior of the Ag electrode cannot solely be a sufficient condition for achieving better catalytic activity but undoubtedly, it is an important and necessary criterion. We proposed Ti as one viable candidate to isolate the work function effect. Future support electrode selection may take advantage of both lattice mismatch and work function difference to control the reduction of organohalides with 3D structures. Our current work thus put forward a systemic approach to aid in guiding experimental efforts in the design of more electrocatalytically active electrode heterostructures for organohalide reduction.

Conclusions:

In this work, we have investigated the impact of surface adsorption on the two-electron reduction of halothane, bromobenzene, and benzyl bromide on Ag and Ag-coated electrodes. We first connected the half-wave potential with the molecular reduction potential and the overpotential induced by the charge transfer rate and surface adsorption coefficient. The DFT-calculated molecular reduction potentials, especially the first electron reduction process, which facilitates subsequent C-Br bond cleavage, are overall in reasonable agreement with the experimental values recorded for Ag surfaces due to the sufficient electrocatalytic activity of the silver electrode.

To further design Ag-coated support electrodes, we examined support electrodes of Au, Bi, Pt, and Ti, both in their freestanding forms and heterostructures with various thicknesses of the deposited Ag layers. The results showed even a monolayer of Ag can dramatically shift the adsorption energy of an otherwise 'inert' (e.g., Pt) or less active electrode (e.g., Bi) to a more Ag-like. The adsorption

and dissociation energies and charge transfer of the halothane, bromobenzene, and benzyl bromide on these electrode surfaces were examined to establish key descriptors that control the adsorption energies of these species on the electrode surfaces. These specific descriptors include (i) molecular geometry, (ii) lattice mismatch between the support and working electrodes, (iii) work function differences between the support and working electrodes, and (iv) explicit solvation.

The flat-lying aromatic molecules, bromobenzene and benzyl bromide, are much less sensitive (<0.1 eV and <0.3 eV change for molecular and dissociated adsorption energy, respectively) to lattice strains. Their adsorption energy change correlated well with the work function change on Ag-deposited metal surfaces compared to pure Ag electrodes. Thus, the maximum change (~1 eV) of dissociated adsorption energy was found on Ti support, which has a smaller work function than Ag, thus making the Ag surface more negative and electron donating by forming the heterogeneous interface. In comparison, linear halothane is more sensitive to the lattice strain of Ag due to its prismatic upright adsorption state, and simply stretching the Ag lattice by 4.61% can decrease halothane dissociative adsorption energy by ~1.0 eV. Thus, their adsorption energy on Agdeposited metal supports does not show a clear trend due to the combining influence of lattice mismatching and work function change. However, for the Ti support, which has almost no lattice mismatch (-0.04 %) with respect to our working Ag electrode, the work function effect will increase the adsorption energy of halothane by ~1.1 eV. Thus, it is reasonable to conclude that the surface of Ag becomes far more electron donating and vulnerable to adsorption when heterostructures are formed with Ti. We further show that solvent effects systematically decrease the tendency of electrode surface to bind molecules, thus conclusions related to lattice and work function mismatch between the support and working electrode should still hold. We believe, our proposed criteria and design rules for choosing support electrodes in the bilayer electrode format, can readily guide experimentalists to able to finetune the electron donating ability of the Ag surface which in turn can dictate the catalytic activity of the working electrode.

Supporting Information:

Methodologies and computational details; detailed re-derivation of half-wave potential ($E_{1/2}$) as an explicit function of standard reduction potential (E^0); study of surface coverage; Bader charge analysis; calculated work function of different Ag/metal bilayer electrodes.

Acknowledgment

This work was supported by the NSF Center for Synthetic Organic Electrochemistry, CHE-2002158.

Data Availability

The first-principles computational results for all the adsorption energies are available in the NOMAD repository at https://doi.org/10.17172/NOMAD/2023.07.05-1.

References:

- (1) Qin, S.; Lei, C.; Wang, X.; Chen, W.; Huang, B. Electrocatalytic Activation of Organic Chlorides via Direct and Indirect Electron Transfer Using Atomic Vacancy Control of Palladium-Based Catalyst. *Cell Rep Phys Sci* **2022**, *3* (1), **100713**.
- (2) Dong, X.; Roeckl, J. L.; Waldvogel, S. R.; Morandi, B. Merging Shuttle Reactions and Paired Electrolysis for Reversible Vicinal Dihalogenations. *Science*, **2021**, *371*, 507-514.
- (3) Neukermans, S.; Vorobjov, F.; Kenis, T.; De Wolf, R.; Hereijgers, J.; Breugelmans, T. Electrochemical Reduction of Halogenated Aromatic Compounds at Metal Cathodes in Acetonitrile. *Electrochim. Acta* **2020**, *332*, **135484**.
- (4) Isse, A. A.; Arnaboldi, S.; Durante, C.; Gennaro, A. Electrochemical Reduction of Organic Bromides in 1-Butyl-3-Methylimidazolium Tetrafluoroborate. *J. Electroanal. Chem.*, **2017**, *804*, 240–247.
- (5) Muthukrishnan, A.; Boyarskiy, V.; Sangaranarayanan, M. V.; Boyarskaya, I. Mechanism and Regioselectivity of the Electrochemical Reduction in Polychlorobiphenyls (PCBs): Kinetic Analysis for the Successive Reduction of Chlorines from Dichlorobiphenyls. *J. Phys. Chem. C*, **2012**, *116* (1), 655–664.
- (6) Lai, A.; Aulenta, F.; Mingazzini, M.; Palumbo, M. T.; Papini, M. P.; Verdini, R.; Majone, M. Bioelectrochemical Approach for Reductive and Oxidative Dechlorination of Chlorinated Aliphatic Hydrocarbons (CAHs). *Chemosphere* **2017**, *169*, 351–360.
- (7) Huang, B.; Isse, A. A.; Durante, C.; Wei, C.; Gennaro, A. Electrocatalytic Properties of Transition Metals toward Reductive Dechlorination of Polychloroethanes. *Electrochim. Acta* **2012**, *70*, 50–61.
- (8) Huang, B.; Li, J.; Cao, X.; Zhu, Y.; Chen, W.; Lei, C. Electrochemical Reduction of P-Chloronitrobenzene (p-CNB) at Silver Cathode in Dimethylformamide. *Electrochim. Acta* **2019**, *296*, 980–988.
- (9) Rondinini, S.; Vertova, A. Electrocatalysis on Silver and Silver Alloys for Dichloromethane and Trichloromethane Dehalogenation. *Electrochim. Acta* **2004**, *49* (22–23), 4035–4046.
- (10) Durante, C.; Isse, A. A.; Sandonà, G.; Gennaro, A. Electrochemical Hydrodehalogenation of Polychloromethanes at Silver and Carbon Electrodes. *Appl Catal B* **2009**, *88* (3–4), 479–489.
- (11) Chen, Y. L.; Weng, T. W.; Cai, Z. Y.; Shi, H.; Wu, T. R.; Wu, D. Y.; Oleinick, A.; Svir, I.; Mao, B. W.; Amatore, C.; Tian, Z. Q. A DFT and SERS Study of Synergistic Roles of Thermodynamics and Kinetics during the

- Electrocatalytic Reduction of Benzyl Chloride at Silver Cathodes. *J. Electroanal. Chem.*, **2022**, *914*, **116267**.
- (12) Röckl, J. L.; Pollok, D.; Franke, R.; Waldvogel, S. R. A Decade of Electrochemical Dehydrogenative C,C-Coupling of Aryls. *Acc Chem Res* **2020**, *53* (1), 45–61.
- (13) Siu, J. C.; Fu, N.; Lin, S. Catalyzing Electrosynthesis: A Homogeneous Electrocatalytic Approach to Reaction Discovery. *Acc Chem Res* **2020**, *53* (3), 547–560.
- (14) Zuo, K.; Huang, X.; Liu, X.; Gil Garcia, E. M.; Kim, J.; Jain, A.; Chen, L.; Liang, P.; Zepeda, A.; Verduzco, R.; Lou, J.; Li, Q. A Hybrid Metal—Organic Framework—Reduced Graphene Oxide Nanomaterial for Selective Removal of Chromate from Water in an Electrochemical Process. *Environ Sci Technol* 2020, 54 (20), 13322–13332.
- (15) Jiang, G.; Lan, M.; Zhang, Z.; Lv, X.; Lou, Z.; Xu, X.; Dong, F.; Zhang, S. Identification of Active Hydrogen Species on Palladium Nanoparticles for an Enhanced Electrocatalytic Hydrodechlorination of 2,4-Dichlorophenol in Water. *Environ. Sci. Technol.*, **2017**, *51* (13), 7599-7605.
- (16) Heard, D. M.; Lennox, A. J. J. Electrode Materials in Modern Organic Electrochemistry. *Angew. Chem. Int. Ed.*, **2020**, *59*, 18866.
- (17) Brudzisz, A.; Sulka, G. D.; Brzózka, A. A Facile Approach to Silver Nanowire Array Electrode Preparation and Its Application for Chloroform Reduction. *Electrochim. Acta*, **2020**, *362*, **137110**.
- (18) Huang, Y. F.; Wu, D. Y.; Wang, A.; Ren, B.; Rondinini, S.; Tian, Z. Q.; Amatore, C. Bridging the Gap between Electrochemical and Organometallic Activation: Benzyl Chloride Reduction at Silver Cathodes. *J. Am. Chem. Soc.*, **2010**, *132* (48), 17199–17210.
- (19) Langmaier, J.; Samec, Z. Electrocatalytic reduction of halothane. *J. Electroanal. Chem.*, **1996**, *402*, 107-113.
- (20) Xu, Y.; Yao, Z.; Mao, Z.; Shi, M.; Zhang, X.; Cheng, F.; Yang, H. Bin; Tao, H. bing; Liu, B. Single-Ni-Atom Catalyzes Aqueous Phase Electrochemical Reductive Dechlorination Reaction. *Appl Catal B* 2020, 277, 119057.
- (21) Liu, R.; Zhao, H.; Zhao, X.; He, Z.; Lai, Y.; Shan, W.; Bekana, D.; Li, G.; Liu, J. Defect Sites in Ultrathin Pd Nanowires Facilitate the Highly Efficient Electrochemical Hydrodechlorination of Pollutants by H* _{ads}. *Environ Sci Technol* **2018**, *52* (17), 9992–10002.
- (22) Lou, Z.; Zhou, J.; Sun, M.; Xu, J.; Yang, K.; Lv, D.; Zhao, Y.; Xu, X. MnO2 Enhances Electrocatalytic Hydrodechlorination by Pd/Ni Foam Electrodes and Reduces Pd Needs. *Chem. Eng. J.*, **2018**, *352*, 549–557.
- (23) Rong, H.; Cai, S.; Niu, Z.; Li, Y. Composition-Dependent Catalytic Activity of Bimetallic Nanocrystals: AgPd-Catalyzed Hydrodechlorination of 4-Chlorophenol. *ACS Catal* **2013**, *3* (7), 1560–1563.
- (24) Fang, L.; Xu, C.; Zhang, W.; Huang, L.-Z. The Important Role of Polyvinylpyrrolidone and Cu on Enhancing Dechlorination of 2,4-Dichlorophenol by Cu/Fe Nanoparticles: Performance and Mechanism Study. *Appl Surf Sci* **2018**, *435*, 55–64.

- (25) Hasselmann, T.; Misimi, B.; Boysen, N.; Zanders, D.; Wree, J.; Rogalla, D.; Haeger, T.; Zimmermann, F.; Brinkmann, K. O.; Schädler, S.; Theirich, D.; Heiderhoff, R.; Devi, A.; Riedl, T. Silver Thin-Film Electrodes Grown by Low-Temperature Plasma-Enhanced Spatial Atomic Layer Deposition at Atmospheric Pressure. *Adv Mater Technol* **2023**, *8* (1), 2200796.
- (26) Oh, S.; Park, Y. S.; Park, H.; Kim, H.; Jang, J. H.; Choi, I.; Kim, S.-K. Ag-Deposited Ti Gas Diffusion Electrode in Proton Exchange Membrane CO2 Electrolyzer for CO Production. *J. Ind. Eng. Chem.*, **2020**, *82*, 374–382.
- (27) Guo, J.; Liu, H.; Li, D.; Wang, J.; Djitcheu, X.; He, D.; Zhang, Q. A Minireview on the Synthesis of Single Atom Catalysts. *RSC Adv* **2022**, *12* (15), 9373–9394.
- (28) Choi, J. II; Abdelhafiz, A.; Buntin, P.; Vitale, A.; Robertson, A. W.; Warner, J.; Jang, S. S.; Alamgir, F. M. Contiguous and Atomically Thin Pt Film with Supra-Bulk Behavior Through Graphene-Imposed Epitaxy. *Adv Funct Mater* **2019**, *29* (46), 1902274.
- (29) Zhou, M.; Bao, S.; Bard, A. J. Probing Size and Substrate Effects on the Hydrogen Evolution Reaction by Single Isolated Pt Atoms, Atomic Clusters, and Nanoparticles. *J. Am. Chem. Soc.*, **2019**, *141* (18), 7327–7332.
- (30) Zhou, M.; Dick, J. E.; Bard, A. J. Electrodeposition of Isolated Platinum Atoms and Clusters on Bismuth—Characterization and Electrocatalysis. *J. Am. Chem. Soc.*, **2017**, *139* (48), 17677–17682.
- (31) Huang, B.; Zhu, Y.; Li, J.; Zeng, G.; Lei, C. Uncovering the Intrinsic Relationship of Electrocatalysis and Molecular Electrochemistry for Dissociative Electron Transfer to Polychloroethanes at Silver Cathode. *Electrochim Acta* **2017**, *231*, 590–600.
- (32) Wang, A.; Huang, Y. F.; Sur, U. K.; Wu, D. Y.; Ren, B.; Rondinini, S.; Amatore, C.; Tian, Z. Q. In Situ Identification of Intermediates of Benzyl Chloride Reduction at a Silver Electrode by SERS Coupled with DFT Calculations. *J Am Chem Soc* **2010**, *132* (28), 9534–9536.
- (33) Nørskov, J. K.; Bligaard, T.; Rossmeisl, J.; Christensen, C. H. Towards the Computational Design of Solid Catalysts. *Nat. Chem.*, **2009**, *1*, 37–46.
- (34) Nørskov, J. K.; Bligaard, T.; Logadottir, A.; Bahn, S.; Hansen, L. B.; Bollinger, M.; Bengaard, H.; Hammer, B.; Sljivancanin, Z.; Mavrikakis, M.; Xu, Y.; Dahl, S.; Jacobsen, C. J. H. Universality in Heterogeneous Catalysis. *J Catal* **2002**, *209* (2), 275–278.
- (35) Toulhoat, H.; Raybaud, P. Prediction of Optimal Catalysts for a given Chemical Reaction. *Catal Sci Technol* **2020**, *10* (7), 2069–2081.
- (36) Marenich, A.; Ho, J.; Coote, M. et al. Computational electrochemistry: prediction of liquid-phase reduction potentials. *Phys. Chem. Chem. Phys.* **2014**, 16(29) 15068-15106.
- (37) Chen, B. W. J.; Xu, L.; Mavrikakis, M. Computational Methods in Heterogeneous Catalysis. *Chem Rev* **2021**, *121* (2), 1007–1048.
- (38) Polishchuk, I.; Ranade, P.; King, T.; Hu, C. Dual work function metal gate CMOS technology using metal interdiffusion. *IEEE Electron Device Lett.*, **2001**, *22* (9), 444-446.

- (39) Olubosede, O.; Afolabi, O.M. et al. Comparison of Calculated Work Function of Metals Using Metallic Plasma Model with Stabilized Jellium, Ab-Initio Approach and Experimental Values *Appl. Phys. Res.* **2011**, 3(2).
- (40) Giesen, K.; Hage, F.; Himpsel, F. J.; Riess, H. J.; Steinmann, W. Binding Energy of Image-Potential States: Dependence on Crystal Structure and Material. *Phys Rev B* **1987**, *35* (3), 971–974.
- (41) Derry, G. N.; Kern, M. E.; Worth, E. H. Recommended Values of Clean Metal Surface Work Functions. *J. Vac. Sci. Technol., A*, **2015**, *33* (6), 060801.
- (42) Beasley, C.; Kumaran Gnanamani, M.; Santillan-Jimenez, E.; Martinelli, M.; Shafer, W. D.; Hopps, S. D.; Wanninayake, N.; Kim, D. Effect of Metal Work Function on Hydrogen Production from Photocatalytic Water Splitting with MTiO ₂ Catalysts. *ChemistrySelect*, **2020**, *5* (3), 1013–1019.
- (43) Lee, A. F.; Chang, Z.; Hackett, S. F. J.; Newman, A. D.; Wilson, K. Hydrodebromination of Bromobenzene over Pt(111). *J. Phys. Chem. C*, **2007**, *111* (28), 10455–10460.
- (44) Isse, A. A.; De Giusti, A.; Gennaro, A.; Falciola, L.; Mussini, P. R. Electrochemical Reduction of Benzyl Halides at a Silver Electrode. *Electrochim. Acta* **2006**, *51* (23), 4956–4964.
- (45) Frisch, M. J. et al. Gaussian 09, Revision A.02. Gaussian Inc. Wallingford CT.
- (46) Wu, Q.; McDowell, M.; Qi, Y. Effect of the Electric Double Layer (EDL) in Multicomponent Electrolyte Reduction and Solid Electrolyte Interphase (SEI) Formation in Lithium Batteries. *J. Am. Chem. Soc.*, **2023**, 145(4), 2473-2484.
- (47) Kresse, G.; Hafner, J. Ab Initio Molecular Dynamics for Liquid Metals. Phys Rev B 1993, 47 (1), 558–561.
- (48) Kresse, G.; Furthmüller, J. Efficiency of Ab-Initio Total Energy Calculations for Metals and Semiconductors Using a Plane-Wave Basis Set. *Comput Mater Sci* **1996**, *6* (1), 15–50.
- (49) Kresse, G.; Furthmüller, J. Efficient Iterative Schemes for *Ab Initio* Total-Energy Calculations Using a Plane-Wave Basis Set. *Phys Rev B* **1996**, *54* (16), 11169–11186.
- (50) Dassault Systemes: San Diego, 2020. Dassault Systemes BIOVIA. Material Studio.
- (51) Bellomunno, C.; Bonanomi, D.; Falciola, L.; Longhi, M.; Mussini, P. R.; Doubova, L. M.; Di Silvestro, G. Building up an Electrocatalytic Activity Scale of Cathode Materials for Organic Halide Reductions. *Electrochim. Acta* **2005**, *50* (11), 2331–2341.
- (52) Bogojeski, M.; Vogt-Maranto, L.; Tuckerman, M.E. et al. Quantum chemical accuracy from density functional approximations via machine learning. *Nat. Commun.*, **2020**, *11*, 5223.
- (53) Almeida, M. O.; Kolb, M. J.; R. V. Lanza, M., Illas, F.; Calle-Vallejo, F. Gas-Phase Errors Affect DFT-Based Electrocatalysis Models of Oxygen Reduction to Hydrogen Peroxide. *ChemElectroChem* **2022**, *9*, e202200210.
- (54) Ooka, H.; Huang, J.; Exner, K. S. The Sabatier Principle in Electrocatalysis: Basics, Limitations, and Extensions. *Frontiers in Energy Research*, **2021**, *9*, 654460.

- (55) Phongpreecha, T.; Liu, J.; Hodge, D. B.; Qi, Y. Adsorption of Lignin β-O-4 Dimers on Metal Surfaces in Vacuum and Solvated Environments. *ACS Sustain Chem Eng* **2019**, *7* (2), 2667–2678.
- (56) Logadottir, A.; Rod, T. H.; Nørskov, J. K.; Hammer, B.; Dahl, S.; Jacobsen, C. J. H. The Brønsted-Evans-Polanyi Relation and the Volcano Plot for Ammonia Synthesis over Transition Metal Catalysts. *J Catal* **2001**, *197* (2), 229–231.